

TWO-LEVEL HOMOGENIZATION METHOD FOR COATED INCLUSION PROBLEM IN ELASTICITY

Dilek Güzel*
Middle East Technical University
Ankara, Turkey
TU Dortmund, Institute of Mechanics
Dortmund, Germany

Ercan Gürses†
Middle East Technical University
Ankara, Turkey

ABSTRACT

Polymer nanocomposites are materials which have polymer matrices and nano-scale reinforcement elements. Other than the matrix and the reinforcement element, another phase, interphase, in nanocomposite systems has been observed and some of the property enhancement or deficiency has been attributed to this phase. The aim of this study is to propose a new homogenization approach to model the polymer nanocomposites with coated inclusions. It is important to model the interphase and obtain the effective composite properties accordingly. The proposed approach is based on a replacement of the coated inclusion (inclusion+interphase) with an effective inclusion using computational homogenization, i.e., finite element method, at the first level, and obtaining the macroscopic response using the micromechanics-based Double-Inclusion method at the second level. This method aims to model load transfer between the matrix and the reinforcement element through the interphase in a correct way. The proposed approach is also extended to non-spherical inclusions.

INTRODUCTION

Polymer nanocomposites are materials which have polymer matrices and nano-scale reinforcement elements. Different from classical, conventional composites, nanocomposites exhibit some phenomena that can be explained by the nano-scale nature of the material [Bhattacharya et al., 2008]. Therefore, new theoretical principles and different experimental techniques are needed in order to understand the behavior of this new class of composites. In the 1980s, Toyota Central Research and Development Laboratories published and filed patents for polymer-clay nanocomposites, which were accepted as the pioneer works in polymer matrix nanocomposite research. There are many challenging problems in the area, such as preparation, synthesis, processing, and characterization of nanocomposites. The uses of polymer nanocomposites in aerospace structures have a great potential and a significant effect on design and applications. Polymer nanocomposites are expected to have multifunctional properties which increases the number of practical applications in aerospace industries.

*Research Assistant in TU Dortmund, Institute of Mechanics Email: dilek.guezel@tu-dortmund.de

†Assoc. Prof. in Department of Aerospace Engineering, Email: gurses@metu.edu.tr

Other than the matrix and the reinforcement element, another phase in nanocomposite systems has been observed and some of the property enhancement or deficiency has been attributed to this phase. The third phase in the composite system is known as the interphase. Since exploration of this phase, characterization and understanding of the interphase became very important in nanocomposite research. The local properties of polymer nanocomposites are not easy to distinguish since the length scale is very small and characterization at the nano-scale is not a simple procedure. Macroscopic behavior of nanocomposites can be deduced by homogenization of a representative volume element in many different ways. Homogenization of two-phase composites is a common approach to understand material behavior. Instead of the local stress and strain results, an effective behavior can be obtained through homogenization.

Homogenization theory is well-established and well-researched area for analyzing heterogeneous materials. The effective or homogenized properties of a heterogeneous medium can be calculated with different numerical or analytical techniques. In general, every material in nature exhibits heterogeneous behavior at some scale. Particle reinforced composites such as polymer matrix nanocomposites are a typical example for heterogeneous materials. Generally, there are at least two phases, the matrix and the inclusion in these materials. Usually the length scale corresponding to the inclusion is smaller than the length scale corresponding to macrostructure. In order to calculate the effective mechanical properties of heterogeneous materials properly, mechanical properties and volume fractions of each constituent as well as the topology should be taken into account. To increase the overall performance of a polymer nanocomposite system, various efforts have been made. For a simple two-phase composite system, other than matrix and inclusions, the existence of a third phase at the interface of these two-phases has been accepted for many years.

Coated Inclusion Problem

The properties of this mentioned interphase region significantly affect the performance of the composite material. Since the establishment of weak or strong interface interactions between the polymer matrix and the inclusion affects the composite's behavior, it should be taken into account when modeling the composite. Some properties of the interphase can be obtained experimentally [Brune et al., 2016; Tian et al., 2019], or by molecular dynamics and similar simulation methods [Odegard et al., 2005; Kim et al., 2017]. In order to model the macroscopic behavior of nanocomposite materials, it has become a necessity to investigate the general structure and properties of the interphase region.

In order to determine the effective mechanical properties of the n-phase heterogeneous environment, a model called Composite Sphere Assemblage was proposed by Hashin in 1962 [Hashin, 1962]. The Composite Sphere Assemblage is based on Eshelby's well-known analytical results [Eshelby, 1957] and it is a method used to determine the limits of bulk and shear moduli of spherical and cylindrical inclusion problems. In the thin interphase approach proposed by Walpole [Walpole, 1978], the interphase is considered as a very thin layer between the matrix and the reinforcing element. During the determination of the elastic properties of this medium, the interphase is assumed to be absent and the stress distribution and the effective elastic moduli of the n-phase composite are calculated analytically by using Hill's interfacial operators [Hill, 1983]. Later, Benveniste et al. [Benveniste et al., 1989] introduced a micromechanical-based approach using the "average stress in the matrix" concept developed by Mori-Tanaka [Mori and Tanaka, 1973]. Since for high inclusion volume fractions the Mori-Tanaka model does not work properly, another micromechanical-based approach known as the Generalized Self-Consistent Scheme (GSCS) is developed [Herve and Zaoui, 1993; Christensen and Lo, 1979]. In this method, the phase that creates heterogeneity is assumed to be embedded in an environment with effective composite properties. By means of an iterative algorithm, effective thermo-elastic properties of the composite can be calculated. In 1993, the Double-Inclusion model was presented by Hori and Nemat-Nasser [Hori and Nemat-Nasser, 1993]. The Double-Inclusion model is one of

the most well known, accepted and implemented methods by the date. This model deals with the general case of coated ellipsoidal inclusions in an anisotropic medium in which the inter-inclusion interaction is also evaluated. However, the simplifying assumption of uniform strain field inside the coating is still accepted. Furthermore, these approaches have been extended to the other important phenomena, such as viscoelasticity [Schöneich et al., 2017; Honorio et al., 2017], graded interphase [Li, 2000], magneto-electro-elasticity [Dinzart and Sabar, 2011] and piezoelectric (PZT) particles [Hashemi et al., 2010].

METHOD

Friebel et al. [Friebel et al., 2006] proposed two new techniques, two-level and two-step homogenization, for the general solution to the coated inclusion problem. The two-level approach is based on the matrix seeing the inclusion and the interphase, surrounding coating region as a composite structure. Generally, two-level homogenization methods have a replacement procedure at the first level of homogenization. At the first level, the coated inclusion is treated as a two-phase composite and is homogenized using different methods. At the end of the first level, the new effective inclusion is placed inside the matrix, then at the second level the matrix and the effective inclusion can be homogenized in order to model the overall effective composite behavior. The two level homogenization scheme has been implemented by different researchers as a common practice.

Double-Inclusion Model

In this work, the Double-Inclusion model, proposed by Hori and Nemat-Nasser [Hori and Nemat-Nasser, 1993], is used for the proposed homogenization technique and for comparison purposes. In the micromechanics-based model proposed by Hori and Nemat-Nasser [Hori and Nemat-Nasser, 1993], the inclusions and coating phases are assumed to be ellipsoidal. Also, the inclusion and the coating are assumed to be coaxial. The D-I model is not limited to isotropy, elasticity of phases can be anisotropic or isotropic. The elasticity tensor of a multi-phase composite \mathbb{C} is given in (1).

$$\begin{aligned}\mathbb{C} &= \mathbb{C}^{inf} : [\mathbb{I} + (\mathbb{S} - \mathbb{I}) : \Lambda] : [\mathbb{I} + \mathbb{S}\Lambda]^{-1} \\ \Lambda &= \sum_{i=1}^n \phi_i \Lambda_i\end{aligned}\quad (1)$$

where ϕ_i is the volume fraction of i^{th} phase, \mathbb{C}^{inf} is the elasticity tensor of a infinitely extended homogeneous domain, \mathbb{I} is the fourth order identity tensor, \mathbb{S} is the Eshelby tensor for ellipsoidal inclusion Eshelby [1957].

The parameter Λ in (1) should be evaluated for every phase (n-phase). If the elasticity tensor is uniform in each phase, Λ can be expressed as in (2). The D-I model allows the phases to be non-uniform for graded evolution of any of the phases [Li, 2000].

$$\Lambda_i = [(\mathbb{C}^{inf} - \mathbb{C}_i)^{-1} : \mathbb{C}^{inf} - \mathbb{S}]^{-1}\quad (2)$$

In (2), \mathbb{C}_i corresponds to elasticity tensor of the phases.

Homogenization with Finite Element Method

In this study strain controlled (driven) tests (FE simulations) are conducted and uniform displacement boundary condition is applied to the representative volume element (RVE). After obtaining the homogenized stress and strain tensors, effective properties can be obtained. The representative volume element is an important concept for homogenization. Instead of modeling complete microstructure of a material, a finite-sized sample is chosen to analyse the model. This sample is called RVE and it shows the macroscopic behavior of the material. There are some size requirements for a finite-sized sample to be qualified as an RVE.

If the homogenized stress and strain results are known the the effective elasticity tensor $\bar{\mathbb{C}}$ can be obtained. For a general anisotropic linear elastic material, the stress-strain relation in Voigt notation is given in (3)

$$\begin{bmatrix} \sigma_{11} \\ \sigma_{22} \\ \sigma_{33} \\ \sigma_{12} \\ \sigma_{23} \\ \sigma_{13} \end{bmatrix} = \begin{bmatrix} C_{11} & C_{12} & C_{13} & C_{14} & C_{15} & C_{16} \\ & C_{22} & C_{23} & C_{24} & C_{25} & C_{26} \\ & & C_{33} & C_{34} & C_{35} & C_{36} \\ & & & C_{44} & C_{45} & C_{46} \\ & & & & C_{55} & C_{56} \\ & & & & & C_{66} \end{bmatrix} : \begin{bmatrix} \epsilon_{11} \\ \epsilon_{22} \\ \epsilon_{33} \\ 2\epsilon_{12} \\ 2\epsilon_{23} \\ 2\epsilon_{13} \end{bmatrix} \quad (3)$$

For the general case of anisotropic elasticity, the elasticity tensor \mathbb{C} has 81 components (21 of which are independent). Thus, 21 equations are needed to obtain 21 constants. Macroscopic stress tensors are calculated by performing strain-controlled finite element analyses. In order to determine each column of the elasticity matrix given in (3), only one component of the strain tensor is specified to a non-zero value while all the other components are set to zero. By conducting finite element analyses of the six load cases given in (4), the elasticity tensor can be computed.

$$\begin{bmatrix} a & 0 & 0 \\ 0 & 0 & 0 \\ 0 & 0 & 0 \end{bmatrix}, \begin{bmatrix} 0 & 0 & 0 \\ 0 & a & 0 \\ 0 & 0 & 0 \end{bmatrix}, \begin{bmatrix} 0 & 0 & 0 \\ 0 & 0 & 0 \\ 0 & 0 & a \end{bmatrix}, \begin{bmatrix} 0 & a & 0 \\ a & 0 & 0 \\ 0 & 0 & 0 \end{bmatrix}, \begin{bmatrix} 0 & 0 & 0 \\ 0 & 0 & a \\ 0 & a & 0 \end{bmatrix}, \begin{bmatrix} 0 & 0 & a \\ 0 & 0 & 0 \\ a & 0 & 0 \end{bmatrix} \quad (4)$$

In (4) a is a small constant which is taken as 0.05 in computations. Note that, since the behavior is assumed to be linear elastic the value of a does not affect the homogenized moduli computed. For isotropic materials, there are only two independent material parameters, therefore even though general six loading cases give every component of the elasticity tensor one by one, use of only one uniaxial loading is enough. In the current study spherical RVEs with spherical inclusions are considered.

In three-dimensional problems a sphere is chosen as a RVE. Abaqus/Standard is used for the finite element analyses [ABAQUS, 2014]. The geometry, load conditions and boundary conditions are created in Abaqus. In Fig. 1a, a cut-out image of the RVE is shown where red part is the matrix, while green is the interphase and blue is the inclusion. Corresponding two-dimensional view of the mesh is illustrated in Fig. 1b. As seen in Fig. 1b, a structured mesh is used. A linear, 8-noded brick element (C3D8) with full integration is chosen for three-dimensional analyses.

After applying a load case to the RVE, the homogenized stress tensor should be computed. Since a uniform displacement boundary condition is applied to the entire surface of the RVE, the homogenized strain tensor is prescribed. For this purpose, during the finite element analysis of the RVE, the volume of each integration point is also stored. By a simple Python code, the homogenized stress and strain tensors are computed by using the stress and strain tensors at the integration points which is depicted in (5).

$$\begin{aligned} \bar{\boldsymbol{\sigma}} &= \frac{\sum_{i=1}^{\text{NIP}} \boldsymbol{\sigma}_i V_i}{\sum_{j=1}^{\text{NIP}} V_j} \\ \bar{\boldsymbol{\epsilon}} &= \frac{\sum_{i=1}^{\text{NIP}} \boldsymbol{\epsilon}_i V_i}{\sum_{j=1}^{\text{NIP}} V_j} \end{aligned} \quad (5)$$

In (5), $\boldsymbol{\sigma}_i$ and $\boldsymbol{\epsilon}_i$ correspond to the stress and the strain tensors at the integration point i , V_i is the volume of that integration point and NIP is the total number of integration points of the FE model.

The proposed methodology in this article uses a two-level homogenization technique. Two-level technique is a common practice for coated inclusion problems. Forming an *effective inclusion* is

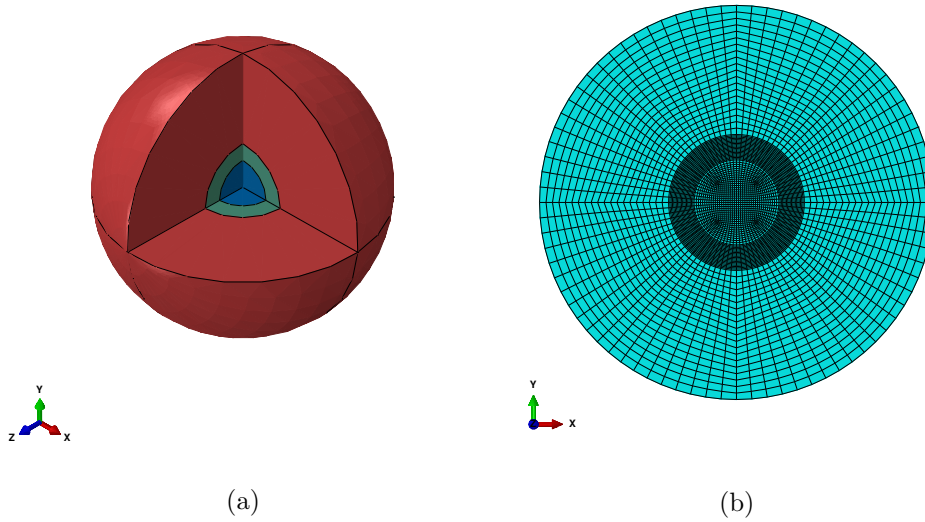


Figure 1: The spherical representative volume element and the corresponding finite element mesh for coated inclusion problem

the main goal at the first level. Then any homogenization technique can be used in the second level to homogenize the obtained two-phase composite. In this study, a two-level technique based on micromechanics and FEA is proposed and the results are reported for elastic and viscoelastic material behavior. The proposed method can be utilized even if constituents are anisotropic or the macroscopic response is anisotropic due to the shape of inclusion.

The method is briefly illustrated in Fig. 2. There are three distinct phases, the matrix (orange), the interphase (blue) and the inclusion (gray). At the first level the interphase and the inclusion are homogenized by using finite element analysis technique and an effective inclusion (dark gray) is obtained. The effective inclusion's elasticity tensor and physical material constants are determined at the end of first level. Then a two-phase composite consisting of a matrix and an effective inclusion is obtained. In the second level the D-I iterative method is used to find the effective properties of two-phase composite. Finally a homogenized, effective material (yellow) is obtained.

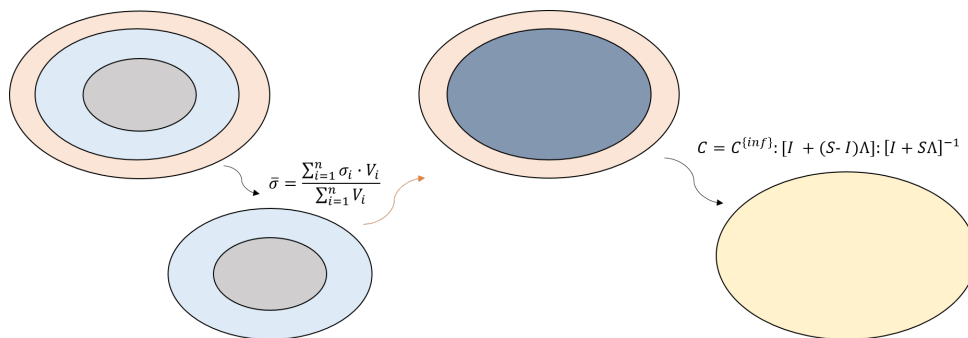


Figure 2: Illustration of proposed two-level homogenization methodology for the coated inclusion problem

An algorithmic chart for the proposed model is presented in Algorithm 1.

Algorithm 1: Proposed methodology for elastic problem

-
- Result:** Effective material properties of three-phase polymer nanocomposite
- 1 Create the geometry with Abaqus for specific volume fraction of inclusion $\phi_{\text{inclusion}}$;
 - 2 Apply six load cases;
 - 3 Perform the following algorithm via Python script in Abaqus PDE;
 - 4 **while** $j \leq \text{load cases}$ **do**
 - 5 **while** $i \leq n$ (*total number of integration points*) **do**
 - 6 $\bar{\sigma} = \frac{\sum_{i=1}^n \sigma_i V_i}{\sum_{i=1}^n V_i}$ $\bar{\varepsilon} = \frac{\sum_{i=1}^n \varepsilon_i V_i}{\sum_{i=1}^n V_i}$
 - 7 **end**
 - 8 $\bar{\mathbb{C}}(,j) = \frac{\bar{\sigma}(,j)}{\bar{\varepsilon}(,j)}$
 - 9 **end**
 - 10 Place the moduli of the effective inclusion into Double-Inclusion method script in Matlab and calculate the homogenized elastic modulus of three-phase composite with an iterative solution;
 - 11 Compute the physical material parameters from the elasticity tensor according to whether the obtained result shows isotropy or not
-

RESULTS AND DISCUSSION

Two cases are studied, namely, the interphase being softer than the matrix and the interphase being stiffer than the matrix. The corresponding Young's modulus for the soft and the stiff interphases are $0.1 \times E_m = 0.25\text{GPa}$ and $10 \times E_m = 25\text{GPa}$. For both cases, $\nu = 0.3$ is chosen. In the micromechanics-based model proposed by Hori and Nemat-Nasser Hori and Nemat-Nasser [1993], the inclusions and coating phases are assumed to be ellipsoidal. Also, the inclusion and the coating are assumed to be coaxial.

Table 1: Material properties for the composite system

Material	Young's modulus E[GPa]	Poisson ratio (ν)
Matrix	2.5	0.34
Interphase	0.25 or 25.0	0.30
Inclusion	1000	0.30

Three-Dimensional Results for Double-Inclusion Model

Fig. 3a proves that, when there is a stiff interphase, the micromechanics-based model is in a good agreement with the three-phase FEA (reference solution). However, when the interphase is softer than the matrix, these models do not match. The D-I model even shows an increasing trend for high volume fractions while the reference solution is monotonously decreasing. It shows that, even though the volume fraction of inclusion is getting higher, due to presence of soft interphase, the overall macroscopic elastic modulus decreases. Therefore, even the trend of the elastic modulus with the volume fraction is different for the D-I model and the reference FE solution. In order to overcome the stress shielding problem for soft interphase and eliminate this mismatch, proposed method is used for three-dimensional geometries as well. The comparison of the proposed method with the D-I method and the reference solution is given in Fig. 3b. The predictions of the proposed method is closer to the reference solution for the stiff interphase case as well.

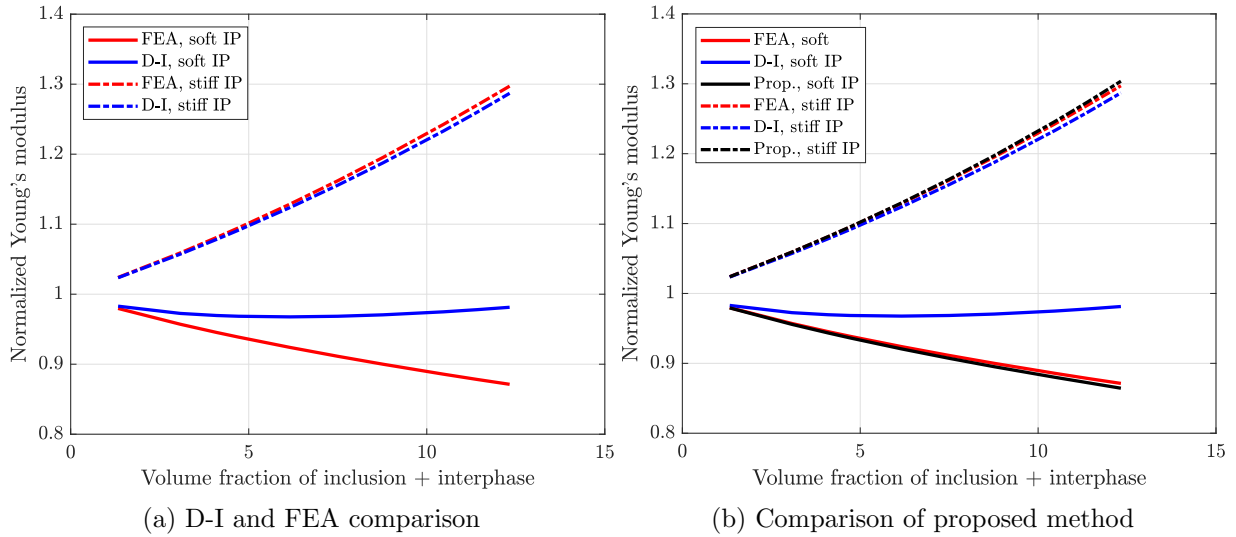


Figure 3: Three-dimensional reference results for thickness t_0 case

Fig. 4 illustrates the cases for which the interphase Young's moduli are set to 0 and ∞ . The first condition corresponds to the case where the load transfer between the matrix and the inclusion is completely prevented. The latter condition corresponds to a rigid interphase. As expected, the soft and the stiff interphase curves are between these limits.

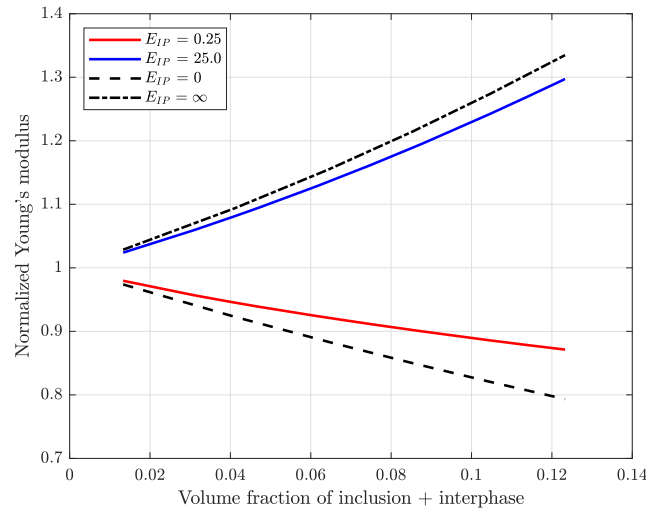


Figure 4: Comparison of the soft and the stiff interphase cases with limit cases.

Variation of Interphase Thickness in Three-Dimensions

In the former section, the proposed method is compared to the reference FEA solution and the micromechanics-based D-I solution for one interphase thickness only. The results show that, by means of a two-level homogenization, a remarkable improvement is achieved. In order to observe how interphase thickness affects the performance of the proposed model, four different interphase thicknesses are chosen, $t_0/2$, $3t_0/4$, t_0 and $5t_0/4$. t_0 is accepted as the reference thickness, which corresponds to 0.6 of radius of inclusion having 0.01 volume fraction. This is chosen as a specified interphase thickness for different volume fractions.

In three-dimensional models even the overall volume fraction of thinnest interphase case is well above the dilute limit. Similar to previous results, for the stiff interphase case three methods,

the three-phase FEA (reference model), the D-I method and the proposed method agree well, see Fig. 5.

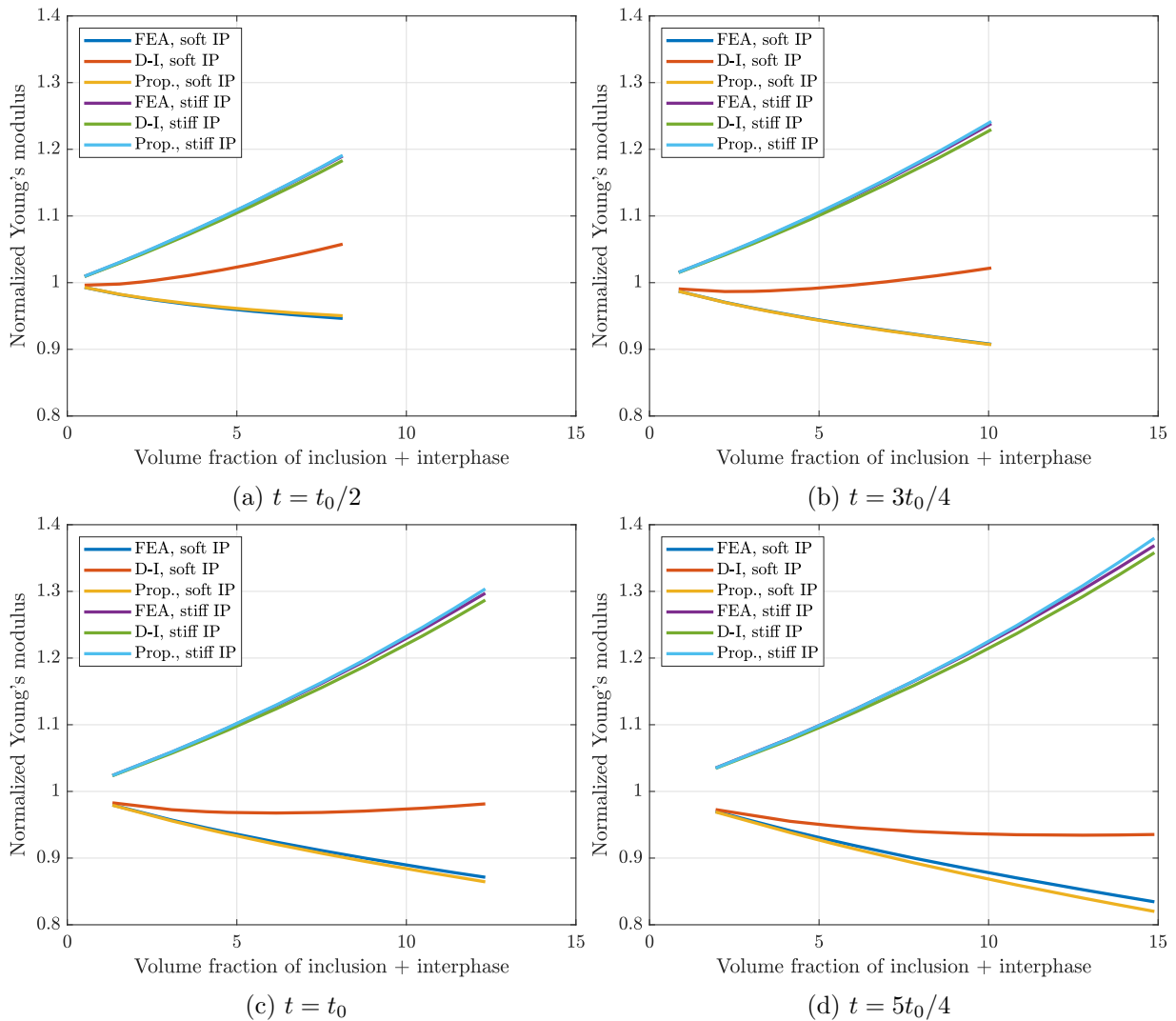


Figure 5: Effect of interphase thickness in three-dimensional problems. Comparison of the proposed method with the D-I method and the FEA

Dilute Limit Violation for Three-Dimensional Problems

To prove the eligibility of the proposed method over dilute limit, higher volume fractions of inclusion and interphase is studied. Fig. 6 indicates that the proposed model works well over dilute limit for the soft interphase case. The discrepancy between the reference solution and the proposed model is also slightly increases. The performance of the methods for the stiff interphase case shows a dependency on the volume fraction. It seems that over the dilute limit, the D-I model and the proposed method do not calculate the effective properties very well. It shows that the two-level homogenization technique may overestimate the homogenized properties of the multi-phase composite. It is known that the D-I and the M-T methods work better in the volume fraction range of 0% – 30%. For really high volume fractions micromechanics-based methods such as the D-I and the M-T methods are not very suitable. This may be an explanation for the discrepancy between the D-I method and the reference solution. However, interesting result here is that the proposed two-level homogenization scheme overestimates both the reference solution and the D-I solution over the dilute limit. Fig. 6 demonstrates that for soft interphase with high volume fractions, proposed method can be performed and calculated effective properties

are very close to reference solution.

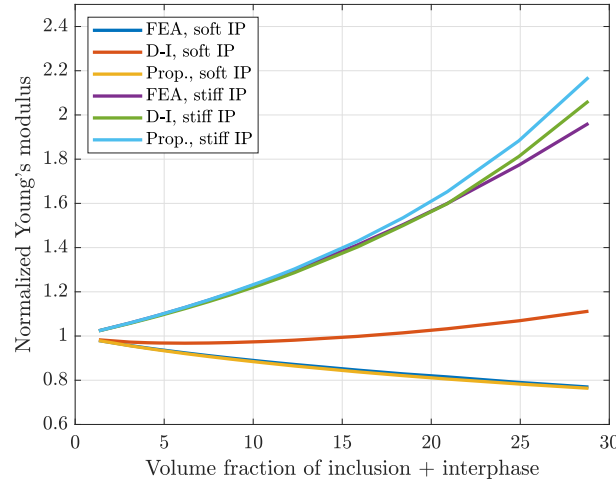


Figure 6: Dilute limit violation in three-dimensions, for thickness, t_0

Extension to Non-Spherical Inclusions: A Short Fiber Reinforced Composite Example

Until this point, the representative volume element (RVE) is chosen as spherical. Furthermore, the inclusion shapes are chosen similarly as spherical. The response of these RVEs exhibit isotropy as long as constituents are isotropic. One of the main advantages of the D-I model is that it is not limited to spherical inclusions only, rather formulations are available for ellipsoidal inclusions as well. Here to demonstrate this capability a transversely isotropic example, an ellipsoidal inclusion in an ellipsoidal RVE is chosen to analyse. This example is analysed in order to show capability of the method to model different geometries. Since sphere is a special case of an ellipsoid, in which all the major and minor radii are the same ($a = b = c$), a general spheroid ($a = b < c$) case is modeled for this purpose. In micromechanics-based methods Eshelby tensor \mathbb{S} is calculated differently depending on the aspect ratio. Here the components of the Eshelby tensor are presented for an ellipsoidal inclusion for an isotropic medium.

$$\begin{aligned}
 S_{1111} &= \frac{3}{8\pi(1-\nu)} a^2 I_{11} + \frac{1-2\nu}{8\pi(1-\nu)} I_1 \\
 S_{1122} &= \frac{1}{8\pi(1-\nu)} b^2 I_{12} + \frac{1-2\nu}{8\pi(1-\nu)} I_1 \\
 S_{1133} &= \frac{1}{8\pi(1-\nu)} c^2 I_{13} + \frac{1-2\nu}{8\pi(1-\nu)} I_1 \\
 S_{1212} &= \frac{a^2 + b^2}{16\pi(1-\nu)} I_{12} + \frac{1-2\nu}{16\pi(1-\nu)} (I_1 + I_2) \\
 S_{1112} &= S_{1223} = S_{1232} = 0
 \end{aligned} \tag{6}$$

In (6) it is assumed that $a > b > c$ where a , b and c are the semi axes of the ellipsoid. Here I terms are defined as standard elliptic integrals as follows.

$$\begin{aligned}
I_1 &= \frac{4\pi abc}{(a^2 - b^2)\sqrt{(a^2 - c^2)}} [F(\theta, k) - E(\theta, k)] \\
I_3 &= \frac{4\pi abc}{(b^2 - c^2)\sqrt{(a^2 - c^2)}} \left[\frac{b\sqrt{(a^2 - c^2)}}{ac} - E(\theta, k) \right] \\
F(\theta, k) &= \int_0^\theta \frac{dw}{(1 - k^2 \sin^2 w)^{1/2}} \\
E(\theta, k) &= \int_0^\theta (1 - k^2 \sin^2 w)^{1/2} dw
\end{aligned} \tag{7}$$

where,

$$\begin{aligned}
\theta &= \arcsin \sqrt{\frac{a^2 - c^2}{a^2}} \\
k &= \sqrt{\frac{a^2 - b^2}{a^2 - c^2}}
\end{aligned} \tag{8}$$

Note that these elliptic integrals should satisfy the conditions given in (9).

$$\begin{aligned}
I_1 + I_2 + I_3 &= 4\pi \\
3I_{11} + I_{12} + I_{13} &= \frac{4\pi}{a^2} \\
3a^2 I_{11} + b^2 I_{12} + c^2 I_{13} &= 3I_1 \\
I_{12} &= \frac{I_2 - I_1}{a^2 - b^2}
\end{aligned} \tag{9}$$

Material properties of the soft interphase case are chosen for illustration, see Table 1. Thus the interphase is the softest of all materials in the system. Furthermore, the thickness is kept constant while the inclusion volume fraction changes from $\phi = 0.01$ to $\phi = 0.05$. A unidirectional fiber alignment is considered and effects of orientation distribution are not investigated. Aspect ratio of fiber is chosen as 20. It is important to note that the thicknesses of the interphase along the longitudinal and the transverse directions are different and depend on the aspect ratio. Aspect ratio is an important variable for fiber reinforced composites. Due to geometry of the fiber and problems related with the mesh generation, 20 is chosen in this study.

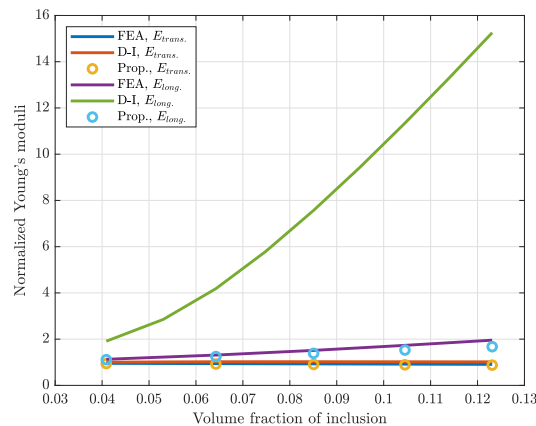


Figure 7: Longitudinal and transverse Young's moduli for single fiber reinforced composite. Comparison of the proposed method and micromechanics based D-I method with reference finite element solution.

Fig. 7 demonstrates that the Young's moduli predictions of the proposed method agrees very well with the reference finite element solution both in longitudinal and transverse directions. It is apparent that the prediction of the D-I method for the longitudinal modulus of the composite is very poor compared to the reference solution. The D-I method also slightly overestimates the transverse modulus and needs an improvement. The need for an improvement can be stated easily for the longitudinal Young's modulus results. However, close up observations demonstrate the overestimation of the D-I method for the transverse modulus as well, see Fig. 8b.

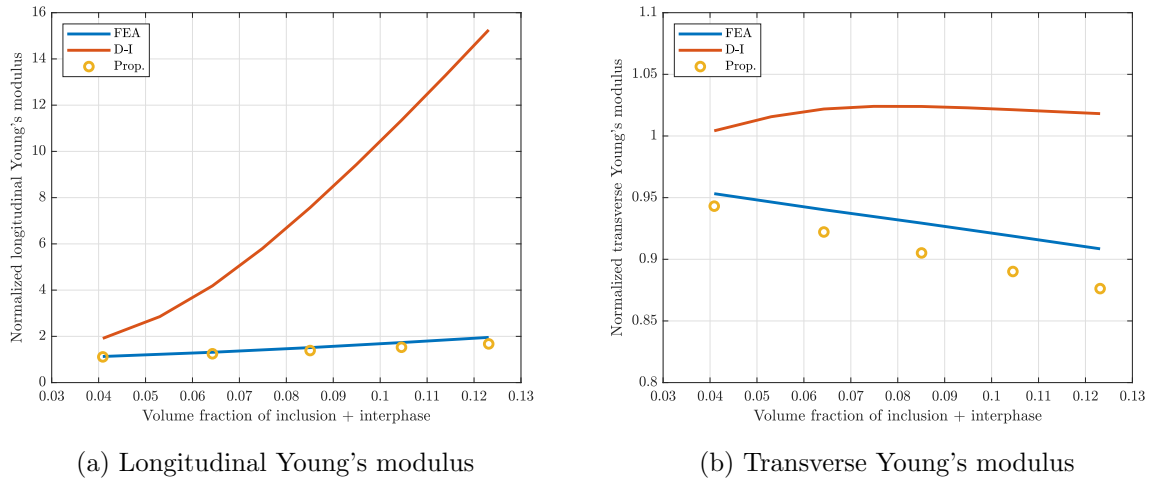


Figure 8: Comparison of the proposed method and micromechanics based D-I method with reference finite element solution.

Close up plots of Fig. 7 are shown in Fig. 8 for the longitudinal and the transverse moduli. As seen in Fig. 8a, the proposed method and the reference solution are in good agreement. By means of a replacement procedure and forming an effective inclusion, overestimation problem of the D-I method resulted due to the soft interphase is prevented. However, the proposed method still slightly underestimates the reference solution. This is also observed for the spherical inclusion case, see Fig. 3b, and therefore is not unexpected. This underestimation becomes more clear when the transverse modulus is compared, see Fig. 8b. But, the performance of the proposed model is still acceptable. As seen in Fig. 8b, the micromechanics-based D-I prediction of transverse modulus behaves very differently. The transverse modulus of the D-I method does not change monotonously with the volume fraction of the inclusion. Therefore, the characteristics of the transverse modulus of FEA is not followed in D-I model.

CONCLUSIONS

In the article, a two-level homogenization method for polymer nanocomposites with coated inclusions is proposed. Depending on the thickness of the interphase, interphase volume fraction may correspond to a significant portion; hence interphase modeling is essential for polymer nanocomposites.

- When there is a soft interphase (softer than the matrix and the inclusion), the load transfer between the matrix and the interphase is prevented. Micromechanics-based *Double-Inclusion* method cannot predict that behavior, as illustrated in Fig. 3b. (In Fig. 3b, blue corresponds to Double-Inclusion results, red corresponds to full-three phase finite element homogenization results and black corresponds to our proposed two-level homogenization approach)
- The proposed method provides a remarkable improvement compared to micromechanics-

based method for the soft interphase case, as illustrated in Fig. 3b. Two-dimensional (circular) and three-dimensional (spherical) RVEs are examined. Different thickness and volume fraction cases, micromechanics-based methods are discussed in the thesis.

- The proposed methodology is extended to non-spherical (ellipsoidal) inclusions, transverse isotropic response is obtained as a result of the proposed approach.

Acknowledgement: This work is supported by the Scientific and Technological Research Council of Turkey (TUBİTAK), Grant No. 218M274.

References

- ABAQUS. *ABAQUS/Standard User's Manual, Version 6.14*. Dassault Systèmes Simulia Corp, United States, 2014.
- Y. Benveniste, G. Dvorak, and T. Chen. Stress fields in composites with coated inclusions. *Mechanics of Materials*, 7(4):305 – 317, 1989. ISSN 0167-6636. doi: [https://doi.org/10.1016/0167-6636\(89\)90021-5](https://doi.org/10.1016/0167-6636(89)90021-5).
- S. N. Bhattacharya, M. R. Kamal, and R. K. Gupta. Application of polymer nanocomposites. In S. N. Bhattacharya, M. R. Kamal, and R. K. Gupta, editors, *Nanocomposites*, pages 339 – 373. Hanser, 2008. ISBN 978-3-446-40270-6. doi: <https://doi.org/10.3139/9783446418523.007>.
- P. F. Brune, G. S. Blackman, T. Diehl, J. S. Meth, D. Brill, Y. Tao, and J. Thornton. Direct measurement of rubber interphase stiffness. *Macromolecules*, 49(13):4909–4922, 2016. doi: [10.1021/acs.macromol.6b00689](https://doi.org/10.1021/acs.macromol.6b00689).
- R. Christensen and K. Lo. Solutions for effective shear properties in three phase sphere and cylinder models. *Journal of the Mechanics and Physics of Solids*, 27(4):315 – 330, 1979. ISSN 0022-5096. doi: [https://doi.org/10.1016/0022-5096\(79\)90032-2](https://doi.org/10.1016/0022-5096(79)90032-2).
- F. Dinzart and H. Sabar. Magneto-electro-elastic coated inclusion problem and its application to magnetic-piezoelectric composite materials. *International Journal of Solids and Structures*, 48(16):2393 – 2401, 2011. ISSN 0020-7683. doi: <https://doi.org/10.1016/j.ijsolstr.2011.04.010>.
- J. D. Eshelby. The determination of the elastic field of an ellipsoidal inclusion, and related problems. *Proceedings of the Royal Society of London. Series A. Mathematical and Physical Sciences*, 241(1226):376–396, 1957. doi: [10.1098/rspa.1957.0133](https://doi.org/10.1098/rspa.1957.0133).
- C. Friebel, I. Doghri, and V. Legat. General mean-field homogenization schemes for viscoelastic composites containing multiple phases of coated inclusions. *International Journal of Solids and Structures*, 43(9):2513 – 2541, 2006. ISSN 0020-7683. doi: <https://doi.org/10.1016/j.ijsolstr.2005.06.035>.
- R. Hashemi, G. Weng, M. Kargarnovin, and H. Shodja. Piezoelectric composites with periodic multi-coated inhomogeneities. *International Journal of Solids and Structures*, 47(21):2893 – 2904, 2010. ISSN 0020-7683. doi: <https://doi.org/10.1016/j.ijsolstr.2010.06.017>.
- Z. Hashin. The Elastic Moduli of Heterogeneous Materials. *Journal of Applied Mechanics*, 29(1):143–150, 03 1962. ISSN 0021-8936. doi: [10.1115/1.3636446](https://doi.org/10.1115/1.3636446).
- E. Herve and A. Zaoui. n-layered inclusion-based micromechanical modelling. *International Journal of Engineering Science*, 31(1):1 – 10, 1993. ISSN 0020-7225. doi: [https://doi.org/10.1016/0020-7225\(93\)90059-4](https://doi.org/10.1016/0020-7225(93)90059-4).

- R. Hill. Interfacial operators in the mechanics of composite media. *Journal of the Mechanics and Physics of Solids*, 31(4):347 – 357, 1983. ISSN 0022-5096. doi: [https://doi.org/10.1016/0022-5096\(83\)90004-2](https://doi.org/10.1016/0022-5096(83)90004-2).
- T. Honorio, B. Bary, J. Sanahuja, and F. Benboudjema. Effective properties of n-coated composite spheres assemblage in an ageing linear viscoelastic framework. *International Journal of Solids and Structures*, 124:1 – 13, 2017. ISSN 0020-7683. doi: <https://doi.org/10.1016/j.ijsolstr.2017.04.028>.
- M. Hori and S. Nemat-Nasser. Double-inclusion model and overall moduli of multi-phase composites. *Mechanics of Materials*, 14(3):189 – 206, 1993. ISSN 0167-6636. doi: [https://doi.org/10.1016/0167-6636\(93\)90066-Z](https://doi.org/10.1016/0167-6636(93)90066-Z).
- B. Kim, J. Choi, S. Yang, S. Yu, and M. Cho. Multiscale modeling of interphase in crosslinked epoxy nanocomposites. *Composites Part B: Engineering*, 120:128 – 142, 2017. ISSN 1359-8368. doi: <https://doi.org/10.1016/j.compositesb.2017.03.059>.
- J. Y. Li. Thermoelastic behavior of composites with functionally graded interphase: a multi-inclusion model. *International Journal of Solids and Structures*, 37(39):5579 – 5597, 2000. ISSN 0020-7683. doi: [https://doi.org/10.1016/S0020-7683\(99\)00227-9](https://doi.org/10.1016/S0020-7683(99)00227-9).
- T. Mori and K. Tanaka. Average stress in matrix and average elastic energy of materials with misfitting inclusions. *Acta Metallurgica*, 21(5):571 – 574, 1973. ISSN 0001-6160. doi: [https://doi.org/10.1016/0001-6160\(73\)90064-3](https://doi.org/10.1016/0001-6160(73)90064-3).
- G. Odegard, T. Clancy, and T. Gates. Modeling of the mechanical properties of nanoparticle/polymer composites. *Polymer*, 46(2):553 – 562, 2005. ISSN 0032-3861. doi: <https://doi.org/10.1016/j.polymer.2004.11.022>.
- M. Schöneich, F. Dinzart, H. Sabar, S. Berbenni, and M. Stommel. A coated inclusion-based homogenization scheme for viscoelastic composites with interphases. *Mechanics of Materials*, 105:89 – 98, 2017. ISSN 0167-6636. doi: <https://doi.org/10.1016/j.mechmat.2016.11.009>.
- C. Tian, G. Chu, Y. Feng, Y. Lu, C. Miao, N. Ning, L. Zhang, and M. Tian. Quantitatively identify and understand the interphase of sio2/rubber nanocomposites by using nanomechanical mapping technique of afm. *Composites Science and Technology*, 170:1 – 6, 2019. ISSN 0266-3538. doi: <https://doi.org/10.1016/j.compscitech.2018.11.020>.
- L. J. Walpole. A coated inclusion in an elastic medium. *Mathematical Proceedings of the Cambridge Philosophical Society*, 83(3):495–506, 1978. doi: [10.1017/S0305004100054773](https://doi.org/10.1017/S0305004100054773).